# Emission Mössbauer spectroscopy study of the $Fe_3O_4(100)$ surface and $Fe_3O_4/MgO(100)$ and $Fe_3O_4/CoO(100)$ interfaces

L. A. Kalev,[1] P. Schurer,[2] and L. Niesen[1]
[1]*Nuclear Solid State Physics, Materials Science Center, University of Groningen, Nijenborg 4, 9747 AG Groningen, The Netherlands*
[2]*Department of Physics, Royal Military College of Canada, P.O. Box 17000, Station Forces, Kingston, Ontario, Canada K7K 7B4*

(Received 11 July 2003; revised manuscript received 25 August 2003; published 16 October 2003)

$^{57}$Co probe atoms were deposited on the surface of $Fe_3O_4(100)$ films grown on MgO(100) substrates. *In situ* emission Mössbauer spectroscopy and reflection high-energy electron-diffraction measurements were performed on the surface after the deposition and after an annealing at 250 °C. After the deposition, the probe atoms are in $Fe^{2+}$ and $Fe^{3+}$ charge states in a disordered atomic arrangement at the surface. They do not participate in the electron-exchange process that takes place in the bulk part of the film. After annealing at 250 °C the probe atoms partly diffuse below the surface. All of the probe atoms now participate in the electron-exchange process. We observed enhanced fluctuations of the spins at and close to the surface at room temperature. Deposition of a MgO layer on top of the magnetite film significantly reduces the spin fluctuations. At 130 K the probe atoms at the $Fe_3O_4/MgO$ interface are in a $Fe^{3+}$ charge state. Deposition of CoO on a magnetite film results in an interface that consists of a cobalt substituted magnetite layer ($Co_xFe_{3-x}O_4$). We estimate the cobalt content of this interface layer to be $0.5 \pm 0.1$.

DOI: 10.1103/PhysRevB.68.165407 PACS number(s): 76.80.+y, 73.20.−r

## I. INTRODUCTION

Recently the growth of thin epitaxial magnetite ($Fe_3O_4$) films by means of $O_2$-assisted molecular-beam epitaxy (MBE) (Refs. 1,2) has made it possible to study the properties of the magnetite film and its surface. The studies on the magnetite surface were motivated by the use of magnetite as a catalyst in inorganic processes[3] and also by the premise that the knowledge of the surface structure can be directly used in the study of $Fe_3O_4/MgO(100)$ and $Fe_3O_4/CoO(100)$ interfaces.[4] It is expected that a magnetite possesses full spin polarization at the Fermi level.[5] In combination with its high ferrimagnetic Néel temperature (858 K), this material is an excellent candidate as ingredient in spin electronic devices. Surprisingly, the experiments on $Fe_3O_4/MgO/Fe_3O_4$ tunnel junctions showed a tunneling magnetoresistance (TMR) effect of only a few percent.[6,7] It was realized that a detailed knowledge of the $Fe_3O_4/MgO$ interface is necessary for the understanding of the spin-polarization performance of magnetite-based tunneling devices. Another class of thin-film systems where knowledge of the interface is of great importance is that of the exchange bias systems. An example of such a system is $Fe_3O_4/CoO$. This system was proposed as an ingredient in all-oxide spin valve devices.[7] The exchange coupling between a ferromagnetic $Fe_3O_4$ film and an antiferromagnetic CoO film, giving rise to exchange biasing, depends sensitively on the interface structure of these two films.

Magnetite has the crystal structure of an inverse spinel. One-third of the iron ions are located in a tetrahedral oxygen environment (*A* sites) and are in the $Fe^{3+}$ charge state. The other two-third of the iron ions have an octahedral oxygen environment (*B* sites). The iron ions on *B* sites can be formally divided into two equal populations of $Fe^{2+}$ and $Fe^{3+}$ ions.

The $Fe_3O_4(100)$ surface is considered polar in terms of the classification introduced by Tasker for ionic or partly ionic materials.[8,9] In the (100) direction $Fe_3O_4$ shows a stacking sequence of planes with opposite and equal charge density. The iron *A*-site planes are positively charged and planes containing the iron *B*-site and oxygen ions are negatively charged. These alternately charged planes produce a dipole moment perpendicular to the surface, which results in the building up of a large electrostatic energy in the material. However, this energy will vanish if the charge on the faces of the crystal is just one-half of that of the alternating layers (autocompensation). This can be done by reconstruction of the surface. A $(\sqrt{2}\times\sqrt{2})R45°$ reconstruction was first observed on natural single crystals by Tarrach *et al.*[10] and subsequently on MBE-grown epitaxial $Fe_3O_4$ films by Voogt *et al.*[11] Two basic models for $Fe_3O_4(100)$ surface reconstruction fulfilling the autocompensation principle were suggested: (i) a half-filled *A*-site surface termination or (ii) a *B*-site surface termination with oxygen vacancies.[12]

At present, the termination of the magnetite film still remains a controversial problem. *B*-site surface termination of a $Fe_3O_4(100)$ film with an ordered array of oxygen vacancies was reported by Stanka *et al.*[13] A study by Chambers *et al.*[14] on a $Fe_3O_4(100)$ film showed that the surface was terminated by a half monolayer of tetrahedral iron. This result was supported by Mijiritskii *et al.*[15] in their low-energy ion scattering study on a thin epitaxial $Fe_3O_4(100)$ film. Also, surface relaxation was observed.[14,15] The top four *A*-*B* interplanar spacings at the surface were found to deviate from their respective bulk values. It was noted that the type of reconstruction critically depends on the sample preparation history[13,14,16,17] that controls the Fe to O ratio on the surface. Surface terminations that violate the autocompensation principle were also reported. Coey *et al.*[18] interpreted their scanning tunneling images in terms of an array of $Fe^{2+}$

 

and $Fe^{3+}$ ions. In a more recent scanning tunneling microscopy study, Mariotto *et al.*[17] observed dimers of $Fe^{2+}$ and $Fe^{3+}$ ions. In earlier thin-film growth studies, only $1\times1$ reflection high-energy electron-diffraction (RHEED) patterns had been observed, corresponding to unreconstructed surfaces.[19,20] An alternative to the reconstruction for removal of the surface polarity was proposed by Noguera *et al.*[21,22] The authors claim that there always exist enough electronic degrees of freedom in a material to reach charge compensation through filling of the surface electronic states on stoichiometric surfaces.

Mössbauer effect spectroscopy (MES) is a widely used method in the study of magnetite and substituted magnetites. MES makes observations on a local atomic scale and provides crucial information needed for a better understanding of the magnetic behavior on a macroscopic scale. Emission Mössbauer spectroscopy (EMS), compared to other surface sensitive methods, has the advantage that it can probe simultaneously chemical, structural, and magnetic properties with submonolayer sensitivity. A peculiarity of EMS on radioactive probe atoms is that the Mössbauer spectrum is basically that of the daughter nucleus ($^{57}$Fe in this case), whereas the site selection of the probe atoms is governed by the chemical properties of the parent atoms ($^{57}$Co). If sufficient charge carriers are available, the charge state of the daughter probe atom will not be different from that of a stable Fe atom. Above the Verwey temperature ($T_V=122$ K) magnetite shows substantial electrical conductivity due to a $3d$ electron exchange between the *B*-site iron ions. At room temperature the electron hopping time between the *B*-site ions is about 3 ns.[23] This is short compared to both the nuclear precession time and the lifetime of the excited state, so that in a Mössbauer spectrum only an effective iron charge state $Fe^{2.5+}$ is observed. As a result, at room temperature, the Mössbauer spectrum of magnetite consists of two components, one from the $Fe^{3+}$ on *A* sites and one from the effective $Fe^{2.5+}$ on *B* sites. Below $T_V$, the electron exchange is suppressed and manifests itself in a decrease of conductivity and the appearance of additional components in the Mössbauer spectrum which are ascribed to $Fe^{2+}$ and $Fe^{3+}$ ions on the *B* sites.[24,25] Decoupling of some of the *B*-site iron ions from the electron-exchange process and the appearance of a $Fe^{3+}$ component was also observed in Mössbauer measurements on nonstoichiometric $Fe_3O_4$ (Refs. 26,27) and on cobalt and lithium substituted magnetites.[28,29]

In the present study we have deposited $^{57}$Co probe atoms by means of the soft-landing technique[30] on the surface of $Fe_3O_4(100)$ thin films grown by $O_2$-assisted MBE on MgO(100). An emission MES study was performed *in situ* in order to characterize the surface of the magnetite film. Subsequently, after growing MgO or CoO on top, the probe atoms are present at the $Fe_3O_4/MgO(100)$ and $Fe_3O_4/CoO(100)$ interfaces, respectively. An EMS study on these samples makes it possible to characterize the two interfaces.

## II. EXPERIMENT AND RESULTS

Magnetite films were grown by the $O_2$-assisted MBE on polished MgO(100) substrates with a size of $10\times10$ mm. The base pressure in the UHV chamber was $2\times10^{-10}$ mbar. Before deposition, the MgO(100) substrates were annealed for 180 min at 650 °C in an oxygen pressure of $1\times10^{-6}$ mbar. The thickness of the films was 10 nm as defined by the RHEED oscillation during growth. During the growth of the films, oxygen was supplied via a leak valve at a distance of 10 cm from the sample. Iron was supplied to the sample by an effusion cell. The temperature of the substrate during growth was 250 °C. The growth rate was 2.25 nm/min. This procedure is known to produce stoichiometric $Fe_3O_4$ films of good quality.[2] At the end of the film deposition the shutters in front of the iron effusion cell and the oxygen supply were simultaneously closed. The heater of the sample holder was switched off and the sample was left to cool down to room temperature after a pressure of $10^{-8}$ mbar in the MBE chamber was obtained. This treatment is expected to produce a half-filled *A*-site surface termination.[14] The sample was transferred *in situ* to the soft-landing UHV chamber. After this transfer the $Fe_3O_4$ surface was checked for contaminations by Auger electron spectroscopy (AES). Only iron and oxygen peaks were found in the AES spectra.

For the soft-landing experiment, $^{57}$Co ions were created in an ion plasma source. The source contained 2 mCi $^{57}$Co in the form of $CoCl_2$. The $^{57}$Co ions were extracted from the plasma with an energy of 50 keV. The radioactive $^{57}$Co beam was separated from all the other masses at the Groningen isotope separator and was further focused and decelerated before entering the soft-landing UHV chamber. The probe atoms were deposited on the sample with an energy from 5 eV to at most 10 eV. The pressure in the UHV chamber during the soft-landing deposition was in the mid $10^{-11}$ mbar range. In our preliminary soft-landing depositions on test samples the profile of the beam spot on the sample was measured by Rutherford backscattering. The maximum coverage of the surface was one $^{57}$Co per magnetite surface unit cell ($0.839\times0.839$ nm$^2$). More details about the soft-landing deposition facility can be found elsewhere.[30,31] This method for deposition of probe atoms on surfaces was previously successfully used, for instance, in the study of the self-diffusion of $^{111}$Ag probe atoms on Ag(100) surfaces.[32] After the soft-landing deposition of the probe $^{57}$Co ions the sample was brought back *in situ* to the MBE system.

Two samples were prepared for the MES investigation in the soft-landing facility. The $Fe_3O_4$ surface of sample 1 was studied at room temperature *in situ* inside the MBE chamber as prepared [$Fe_3O_4/1$ spectrum, Fig. 1(a)] and after annealing for 30 min at 250 °C [$Fe_3O_4/2$ spectrum, Fig. 1(b)]. Subsequently, after the deposition of 6-nm MgO on sample 1 at 250 °C, a MES spectrum was obtained *in situ* [Fig. 1(c)] for studying the $Fe_3O_4/MgO$ interface. This spectrum is identical to the $Fe_3O_4/MgO/1$ spectrum [Fig. 2(a)] obtained *ex situ* for the same $Fe_3O_4/MgO$ sample, apart from the higher line broadening for the *in situ* measurement. For this sample also a $Fe_3O_4/MgO/2$ spectrum was obtained at 130 K [Fig. 2(b)].

In order to study the $Fe_3O_4/CoO$ interface, after soft

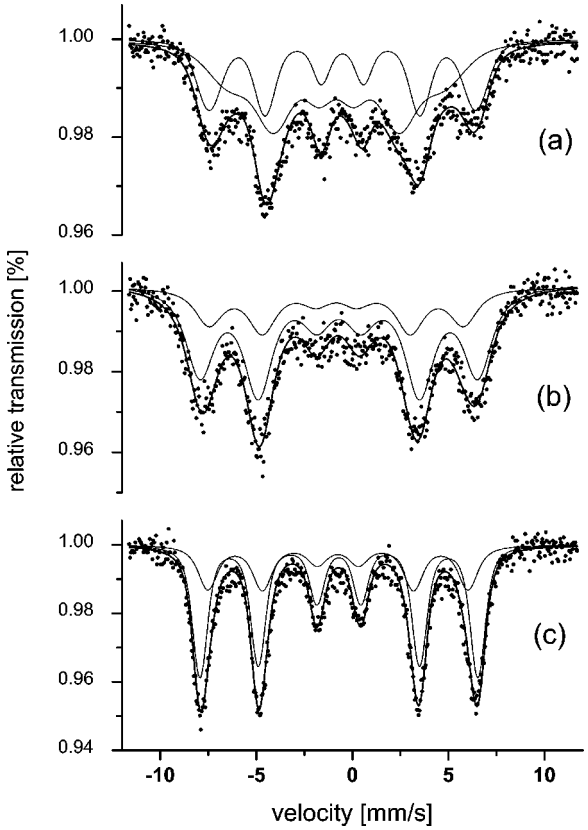


FIG. 1. Emission Mössbauer spectra measured *in situ* at room temperature for $^{57}$Co probe atoms soft landed at the (a) $Fe_3O_4(100)$ surface, (b) $Fe_3O_4(100)$ surface after annealing at 250 °C, and (c) $Fe_3O_4$/MgO interface.

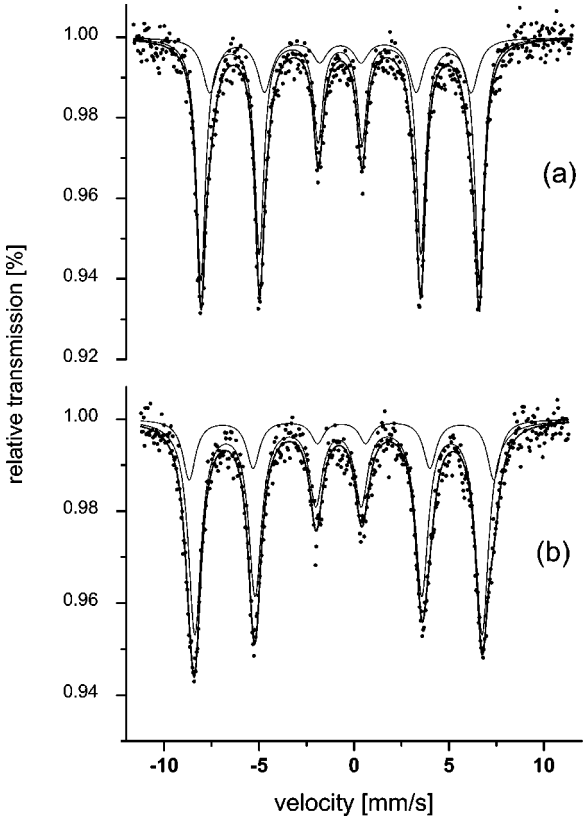


FIG. 2. Emission Mössbauer spectra measured *ex situ* for $^{57}$Co probe atoms present at the $Fe_3O_4$/MgO interface at (a) 295 K and (b) 130 K.

landing of $^{57}$Co probe atoms, a 3-nm CoO film was grown at 250 °C on the $Fe_3O_4$ surface of sample 2. The CoO film was covered by a 6-nm MgO film in order to prevent the oxidation of CoO in air. For this sample we obtained *ex situ* MES spectra, $Fe_3O_4$/CoO/1 at room temperature [Fig. 3(a)] and $Fe_3O_4$/CoO/2 at 130 K [Fig. 3(b)].

The MgO and CoO films were deposited at growth conditions necessary to obtain stoichiometric CoO and MgO films.[33] These conditions are the same as that for the growth of $Fe_3O_4$ except that a somewhat higher growth rate of 3 nm/min is used. The radioactivity of sample 1 and sample 2 were 60 $\mu$Ci and 30 $\mu$Ci, respectively. The mass 57 beam contained 30% of $^{57}$Fe due to the presence of natural iron in the soft-landing system.

The MBE system was equipped with a sample holder facing a beryllium window for performing *in situ* MES investigations. A transducer with a moving single-line Mössbauer absorber made of $Na_4\ ^{57}Fe(CN)_6\cdot 10H_2O$ (95% enriched) was mounted outside the MBE chamber in front of the beryllium window. Vibrations, emanating from the MBE pumping systems producing some line broadening for the *in situ* MES measurements, can be detected by comparing the spectra shown in Figs. 1(c) and 2(a) taken *in situ* and *ex situ*, respectively.

During and after the growth of the $Fe_3O_4$ film we observed a $(\sqrt{2}\times\sqrt{2})R45°$ surface reconstruction in the RHEED image. This reconstruction can be recognized by the appearance of half-order diffraction lines in the zeroth Laue zone. The additional diffraction lines have been observed in other studies and are considered a fingerprint of the surface reconstruction.[12,34] The additional half-order lines disappeared after the soft landing of the probe atoms on the $Fe_3O_4$ surface, as a $1\times1$ surface structure was observed in the RHEED image. It was for this surface condition that the MES spectrum $Fe_3O_4$/1 was collected [Fig. 1(a)]. Afterwards, when the sample was annealed for 30 min at 250 °C, we observed that starting at 150 °C the RHEED image changed back to the original $(\sqrt{2}\times\sqrt{2})R45°$ reconstruction and remained so after the annealing. The spectrum $Fe_3O_4$/2 was collected for this surface condition [Fig. 1(b)].

We performed additional experiments to check if the disappearance of the surface reconstruction is caused by the deposition of $^{57}$Co atoms with 5-eV energy. After preparation of a $Fe_3O_4(100)$ surface in the standard way, the sample was left at room temperature in the UHV chamber for several days. The only RHEED image we observed was of a $(\sqrt{2}\times\sqrt{2})R45°$ surface. Afterwards, natural Fe was deposited on the surface at RT and the RHEED image was continuously monitored. The thermal energy of the Fe atoms coming from the effusion cell was 0.1 eV (1200 °C). At about 20% of a monolayer Fe coverage, the RHEED image transformed from $(\sqrt{2}\times\sqrt{2})R45°$ surface to $1\times1$ and the deposition was stopped. The 20% coverage is comparable with the probe atoms coverage of the soft-landing samples. The sample was

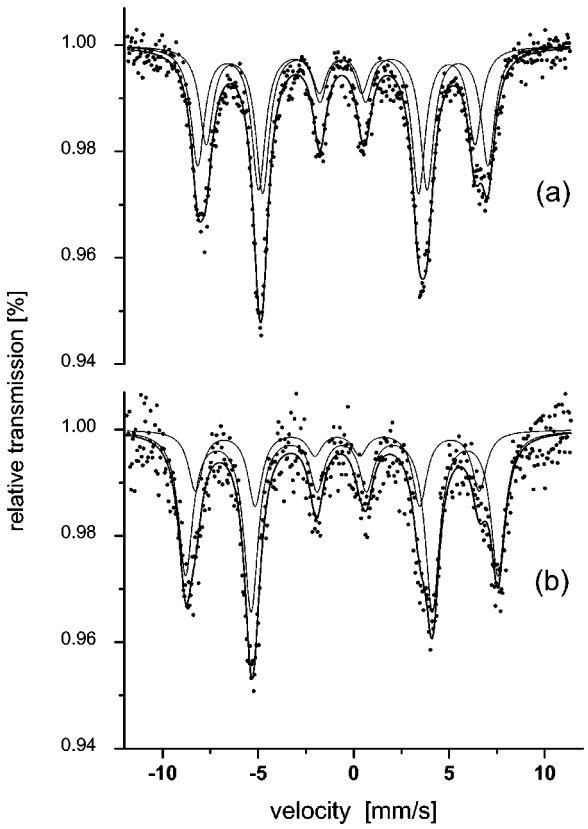


FIG. 3. Emission Mössbauer spectra measured *ex situ* for $^{57}$Co probe atoms present at the $Fe_3O_4$/CoO interface at (a) 295 K and (b) 130 K.

left in UHV conditions for a day and then heated up. The RHEED image transformed back to $(\sqrt{2}\times\sqrt{2})R45°$ at 150 °C. This experiment showed that the change in the surface structure is not caused by the somewhat higher energy of the soft-landed probe atoms. It is worth mentioning that surface structure transformation to $3\times1$ (Refs. 12,35) or $4\times1$ (Ref. 36) has been observed due to diffusion of Mg atoms to the $Fe_3O_4(100)$ film surface from the MgO substrate after annealing at temperatures above 700 K. These results show that the surface symmetry as observed by RHEED can be changed if additional atoms are introduced (or added) to the surface.

Another sample identical to sample 1 was prepared with activity ten times smaller than sample 1 and 70% of $^{57}$Fe in the radioactive beam. The Mössbauer measurements on these two samples produced identical spectra, leading to the conclusion that we can neglect interactions between the probe atoms.

The Mössbauer spectra were processed by a nonlinear least-squares fitting routine. Fits with a varying number of magnetic sextets (components) were attempted. Reasonable fits to the experimental spectra were obtained by a two-component model. Allowing a Gaussian distribution of the magnetic hyperfine field with standard deviation $\sigma$-$B_{hf}$ around an average value, $B_{hf}$ gave appreciable values of $\sigma$-$B_{hf}$ only for the fit of spectrum $Fe_3O_4$/1, where $\sigma$-$B_{hf,S}=3.1$ T and $\sigma$-$B_{hf,B}=1.3$ T. The fitting to the other spectra produced $\sigma$-$B_{hf,S}$ and $\sigma$-$B_{hf,B}$ less than 0.1 T. Therefore, all the spectra except the spectrum $Fe_3O_4$/1 were fitted with Lorentzian line shape. The experimental Lorentzian line width $\Gamma_{exp}$ was obtained after careful examination of the different sources of line broadening such as absorber thickness effects, vibrations in the MBE chamber for the *in situ* measurements, and vibrations in the cryostat for the low-temperature measurements. The values of $\Gamma_{exp}$ for the *in situ*, *ex situ* at RT, and *ex situ* at 130 K measurements were 0.80, 0.48, and 0.63 mm/s, respectively. For the sake of clarity only the additional line broadening $\Delta\Gamma=\Gamma_{tot}-\Gamma_{exp}$ for every particular spectrum is presented in Tables I and II. The area ratio $r=I2/(I1+I3)$ was used as a fitting parameter in each sextet $I1{:}I2{:}I3{:}I3{:}I2{:}I1$. This parameter depends on the orientation angle $\varphi$ between the magnetic hyperfine field and the $\gamma$-*ray* direction via the relation $r=\sin^2\varphi/(1+\cos^2\varphi)$. For in-plane moment alignment $r=1$, and for a perpendicular moment alignment $r=0$.

All the fit results are summarized in Tables I and II for sample 1 and sample 2, respectively. More sophisticated processing of the spectra was not attempted because of the statistical quality of the spectra.

## III. ANALYSIS AND DISCUSSION

The room-temperature hyperfine parameters for bulk magnetite, as reported in the literature are scattered within not so narrow intervals.[26,37,38] As reference data we adopt our conversion electron Mössbauer spectroscopy measurements for a fully $^{57}$Fe enriched 20-nm-thick $Fe_3O_4$ film grown on MgO(100) at the same conditions as the soft-landing samples. At 295 K we have measured $B_{hf,A}=48.4$ T and

TABLE I. Hyperfine parameters derived from the Mössbauer spectra of sample 1. The isomer shifts $\delta$ are relative to $\alpha$-Fe at RT. The intensities $w$, the hyperfine fields $B_{hf}$, the additional line broadening $\Delta\Gamma$, and the area ratios $r$ of the two components $S$ and $B$ are shown. The statistical errors are given in the parentheses.

| Spectrum name | Temperature | Component $S$ | | | | | Component $B$ | | | | |
|---|---|---|---|---|---|---|---|---|---|---|---|
| | | $w_S$ | $\delta_S$ | $B_{hf,S}$ | $\Delta\Gamma_S$ | $r_S$ | $w_B$ | $\delta_B$ | $B_{hf,B}$ | $\Delta\Gamma_B$ | $r_B$ |
| | (K) | (%) | (mm/s) | (T) | (mm/s) | | (%) | (mm/s) | (T) | (mm/s) | |
| $Fe_3O_4$/1 | 295 | 60(3) | 0.84(3) | 35.0(2) | 1.07(8) | 0.92(6) | 40(2) | 0.44(2) | 43.0(2) | 0.51(5) | 0.77(5) |
| $Fe_3O_4$/2 | 295 | 30(3) | 0.71(1) | 41.1(2) | 1.01(6) | 0.79(5) | 70(2) | 0.63(1) | 44.8(1) | 0.63(5) | 0.80(5) |
| $Fe_3O_4$/MgO/1 | 295 | 28(3) | 0.66(1) | 42.7(2) | 0.43(5) | 0.66(4) | 72(2) | 0.64(1) | 45.5(1) | 0.09(4) | 0.62(4) |
| $Fe_3O_4$/MgO/2 | 130 | 25(3) | 0.53(1) | 50.0(1) | 0.24(4) | 0.56(4) | 75(2) | 0.74(1) | 47.0(1) | 0.05(4) | 0.59(4) |

TABLE II. Hyperfine parameters derived from the Mössbauer spectra of sample 2. The isomer shifts $\delta$ are relative to $\alpha$-Fe at RT. The intensities $w$, the hyperfine fields $B_{hf}$, the additional line broadening $\Delta\Gamma$, and the area ratios $r$ of the two components $S$ and $B$ are shown. The statistical errors are given in the brackets.

| Spectrum name | Temperature | Component $B1$ | | | | | Component $B2$ | | | | |
|---|---|---|---|---|---|---|---|---|---|---|---|
| | (K) | $w_{B1}$ (%) | $\delta_{B1}$ (mm/s) | $B_{hf,B1}$ (T) | $\Delta\Gamma_{B1}$ (mm/s) | $r_{B1}$ | $w_{B2}$ (%) | $\delta_{B2}$ (mm/s) | $B_{hf,B2}$ (T) | $\Delta\Gamma_{B2}$ (mm/s) | $r_{B2}$ |
| $Fe_3O_4$/CoO/1 | 295 | 52(2) | 0.50(1) | 47.1(1) | 0.26(2) | 0.83(4) | 48(2) | 0.62(1) | 43.6(1) | 0.21(2) | 0.91(4) |
| $Fe_3O_4$/CoO/2 | 130 | 75(2) | 0.59(1) | 50.6(3) | 0.20(4) | 0.87(4) | 25(3) | 0.75(1) | 46.1(1) | 0.17(4) | 0.89(5) |

$B_{hf,B}=45.3$ T and isomer shifts $\delta_A=0.28$ mm/s and $\delta_B=0.64$ mm/s for the hyperfine parameters of the $A$ and $B$ sites, respectively. The same sample was measured also at 140 K. At this temperature we have observed an increase of 0.10 mm/s in the isomer shift and 2.4 T in the hyperfine field of the $B$-site component.

As we mentioned in the Introduction, the type of reconstruction critically depends on the sample preparation history. Our magnetite films were prepared at the same growth conditions as the ones reported in Refs. 14 and 15, where a half-filled $A$-site surface termination was established. Therefore, we can expect that the $(\sqrt{2}\times\sqrt{2})R45°$ surface symmetry of our $Fe_3O_4$ films corresponds to a half-filled $A$-site surface termination. The isomer shift data of our measurement on the magnetite surface after the soft landing (Table I) shows values greater than $\delta_A=0.28$ mm/s, indicating that there are no $Fe^{3+}$ probe atoms on $A$ sites. If the magnetite surface were $B$-site terminated then after the soft landing the probe atoms would occupy the surface $A$ sites. This would be the easiest way for surface autocompensation. The fact that we do not observe probe atoms on $A$ sites further supports our assumption that the as-prepared magnetite surface is $A$-site terminated.

Figure 1(a) shows the $Fe_3O_4$/1 spectrum acquired from the $Fe_3O_4(100)$ surface after soft-landing of the probe atoms. The spectrum has been fitted with two components $S$ and $B$. The broad component in the spectrum has isomer shift $\delta_S=0.84$ mm/s. A component with isomer shift of $\delta=1.00$ mm/s was found in bulk magnetite measured at 4.2 K and ascribed to a $Fe^{2+}$ charge state.[39] A second-order Doppler-shift reduction of about 0.20 mm/s expected in the isomer shift at RT gives a 0.80 mm/s value for the isomer shift for the $Fe^{2+}$ ions at RT. Therefore, we will interpret the value of $\delta_S$ as originating from $Fe^{2+}$ ions. The other component $B$ has values $\delta_B=0.44$ mm/s and $B_{hf,B}=43$ T. On the basis of the isomer shift we will ascribe this component to $Fe^{3+}$. A component with $\delta=0.39$ mm/s and $B_{hf}=50$ T has been observed in nonstoichiometric magnetite and has been interpreted as arising from $Fe^{3+}$ ions.[26,27]

The values of $\sigma$-$B_{hf}$ for the two components $S$ and $B$ are 3.1 T and 1.6 T, respectively. These broad distributions of the magnetic hyperfine field show that the probe atoms have different atomic environments. As remarked by Noguera,[21] surface diffraction patterns exhibit $1\times1$ symmetry if no ordering on the surface takes place. Therefore, the $1\times1$ surface symmetry as observed in the RHEED image is not due to a bulk surface termination but due to the missing surface order. The RHEED and the MES observations apparently show that the probe atoms are positioned on the surface in a disordered manner. The absence of the 2.5+ charge state, as shown by the MES, leads to the conclusion that these atoms are isolated from the electron-exchange process that exists in the bulk part of the magnetite film.

A quite unexpected evolution of the surface structure is observed after the annealing of the sample. The recovery of the $(\sqrt{2}\times\sqrt{2})R45°$ surface structure is a clear indication that atomic ordering took place during the annealing. The $Fe_3O_4$/2 spectrum acquired after annealing at 250 °C is shown in Fig. 1(b).

The origin of the components observed in the $Fe_3O_4$/2 [Fig. 1(b)] and $Fe_3O_4$/MgO/1 [Fig. 2(a)] spectra becomes clear after comparative analysis of these two spectra. The isomer shifts of the components in the two spectra are equal, within the experimental error, to the isomer shift of $B$ sites' bulk magnetite, 0.64 mm/s, except the somewhat higher value of 0.71 mm/s of component $S$ in the $Fe_3O_4$/2 spectrum. Therefore, we can ascribe these components to a $Fe^{2.5+}$ charge state. The hyperfine field of component $B$ in the $Fe_3O_4$/MgO/1 spectrum is equal to the hyperfine field of 45.5 T observed in bulk magnetite. Therefore, this component originates from probe atoms below the surface having a bulklike $B$-site atomic environment. The $B_{hf,S}$ value of component $S$ can be understood by considering the supertransferred hyperfine field (STHF) contribution to the magnetic hyperfine field. This contribution results from the transfer of electronic spin density from an ion to another via an intermediate ion in a process similar to that of magnetic superexchange.[40] In magnetite and substituted magnetites, this transfer is from the $A$-site ion via the oxygen ion to the $B$-site ion. In this way, any ion substitution of iron on an $A$-site or a missing $A$-site ion can be observed in the Mössbauer spectrum as a reduction of $B_{hf,B}$.

An $A$-site substitution by Mg produces a reduction of $B_{hf,B}$ by 1.3 T.[41] At the $Fe_3O_4$/MgO interface the $B$-site ions will have two $A$-site nearest neighbors less than that in the bulk $Fe_3O_4$. This will amount to a reduction of 2.6 T in the STHF contribution to the total hyperfine field for component $S$ in the $Fe_3O_4$/MgO/1 spectrum. Subtracting the 2.6 T STHF contribution from the bulk hyperfine field of 45.5 T gives 42.9 T, which is consistent with the experimental value of 42.7 T.

In summary, we associate component $S$ with probe atoms in the $B$-site planes at the surface or at the interface and component $B$ with the probe atoms located in the $B$-site

planes closely below the surface of the MgO interface. The intensities of the two components *S* and *B* in the $Fe_3O_4$/2, $Fe_3O_4$/MgO/1, and $Fe_3O_4$/MgO/2 spectra are constant within the experimental error (see Table I). This indicates that the probe atoms conserve their atomic positions after the annealing at 250 °C and during the growth of the MgO film. From the recovery of the surface reconstruction at 150 °C we infer that the surface atoms are quite mobile during the annealing at 250 °C. It may seem surprising that the probe atoms are able to reach *B* layers below the surface. We recall, however, that the probe atoms are still $Co^{2+}$ ions when they diffuse, which means that they will try to reach their preferred thermodynamically stable positions at the *B* sites. The corresponding chemical driving force must be responsible for this diffusion below the surface.

The additional broadening of 1.01 mm/s and 0.63 mm/s in the linewidths of the *S* and *B* components, respectively, in $Fe_3O_4$/2 spectrum could be either due to a distribution of the hyperfine parameters reflecting a different atomic environment of the probe atoms or due to spin-relaxation effects. Actually, both effects could be expected. Surface relaxation of a half-filled *A*-site surface terminated $Fe_3O_4(100)$ surfaces was reported in the literature.[14,15] The first four interlayer spacings are relaxed by $-14\%$, $-57\%$, $-19\%$, and $+29\%$ of the respective bulk values. This surface relaxation substantially modifies Fe-O distances and Fe(*A*)-site-O-Fe (*B*)-site angles, which will result in a variation of the hyperfine parameters and also in a variation of the superexchange interaction between the iron ions on *A* and *B* sites. Together with the reduced number of magnetic neighbors, the latter effect could lead to enhanced fluctuation rates. The increase of $B_{hf,S}$ and $B_{hf,B}$ by 1.6 T and 0.7 T, respectively, after deposition of MgO on the $Fe_3O_4$ surface provides evidence for the fact that the additional line broadening in the $Fe_3O_4$/2 spectrum is to a great extent due to spin-relaxation effects.

The Mössbauer spectrum of the $Fe_3O_4$/MgO interface at 130 K is shown in Fig. 2(b). The hyperfine parameters of component *B* are as expected for bulk magnetite at this temperature. The isomer shift of component *S* is 0.53 mm/s. Extrapolating this value to RT by taking into account the second-order Doppler shift observed in bulk magnetite gives a value of 0.43 mm/s. As was discussed above, this isomer shift corresponds to a $Fe^{3+}$ charge state. This behavior of the *S* component suggests that at 130 K the iron ions at the interface do not take part in the electron-exchange process. Apparently, the interface presents a potential barrier for these carriers. The reason for this potential barrier is probably the presence of divalent *B*-site Mg neighbors of the Fe *B*-site interface atoms, similar to what is observed for Co-substituted $Fe_3O_4$ (see below).

It was suggested that the small TMR effect observed in $Fe_3O_4$/MgO/$Fe_3O_4$ tunnel junctions is caused by a random spin orientation[7] or spin fluctuations[6] close to the $Fe_3O_4$/MgO interface. Spin orientation of 29(5)° out of the film plane was deduced from the area ratio parameter *r* of the $Fe_3O_4$/MgO/1 spectrum in the way described in Sec. II. This spin orientation is close to a spin orientation of 35.3°, which would be produced by a random spin orientation. On the other hand the Mössbauer measurements on thicker fully enriched $Fe_3O_4$ films also produce an average out-of-plane angle of 30° due to the presence of antiphase boundaries and strong antiferromagnetic interactions.[42,43] The small value of $\Delta\Gamma_B = 0.09(5)$ mm/s and the bulklike hyperfine parameters of component *B* strongly suggest that the spins located closely below the $Fe_3O_4$/MgO interface do not behave different from the bulk of the layer. However, the decrease of $\Delta\Gamma_S$, from 0.43 to 0.24 mm/s, when going from 295 K to 130 K provides evidence for the fact that at RT the interface spins fluctuate on a time scale comparable to the time window of the Mössbauer measurement. This is in agreement with the Monte Carlo simulation results of Srinitiwarawong and Gehring[4] They reported reduced surface RT magnetization as a result of the reduced number of magnetic neighbors at the $Fe_3O_4(100)$ surface.

The spectra measured for the $Fe_3O_4$/CoO interface at RT and at 130 K are shown in Fig. 3. The isomer shift of component *B*2 in the two spectra follows the expected values for $Fe^{2.5+}$ for the respective temperatures. Component *B*1 shows isomer shift values $\delta_{B1}$ in between those for $Fe^{2.5+}$ and $Fe^{3+}$ in bulk magnetite. Similar results have been reported by De Grave *et al.*[37] and Persoons *et al.*[44] in their Mössbauer study on cobalt substituted magnetite ($Co_xFe_{3-x}O_4$). Briefly, De Grave *et al.* have resolved two iron sites in the $x<0.4$ substitution range. One due to $Fe^{2.5+}$ ions, which is involved in an electron exchange similar to that taking place in nonsubstituted magnetite and one with a formal charge of $Fe^{2.7+}$. The latter is caused by the presence of $Co^{2+}$ ions on nearest-neighbor *B* sites, which hinders the electron-exchange process. The authors also observed a relative increase in the $Fe^{2.5+}$ intensity with an increase of the temperature and they found that at high temperatures all the *B*-site iron ions are involved in the electron-exchange process. We have shown above, in our measurements on the $Fe_3O_4$ surface and the $Fe_3O_4$/MgO interface that raising the sample temperature to 250 °C is accompanied by a diffusion of the Co probe atoms to *B*-site positions below the surface. We recall that the CoO layer was grown at 250 °C on the $Fe_3O_4$ film. Therefore, it is to be expected that Co atoms diffuse in the magnetite film during the deposition of CoO and form a cobalt substituted magnetite layer between the $Fe_3O_4$ and CoO films. We attribute component *B*1 to iron *B*-site ions with Co *B*-sites nearest neighbors in this layer, and component *B*2 to regular iron *B* sites with only Fe *B*-site nearest neighbors. The increase of the intensity $w_{B1}$ between 295 K and 130 K (Table II) cannot be caused by further diffusion of Co ions below the $Fe_3O_4$/CoO interface. Instead, we attribute this increase to a suppression of the electron-exchange process at low temperatures, as it was observed in bulk $Co_xFe_{3-x}O_4$. In Ref. 44 a linear relationship between the isomer shift and the cobalt content *x* in $Co_xFe_{3-x}O_4$ single crystals was established. Based on this relationship we can roughly estimate the cobalt content of the cobalt substituted magnetite layer to be $x = 0.5 \pm 0.1$.

## IV. SUMMARY AND CONCLUSIONS

We present an experiment where $^{57}Co$ probe atoms have been used in an emission Mössbauer spectroscopy study of

surfaces and interfaces. In particular, we present here a study of the $Fe_3O_4(100)$ surface and $Fe_3O_4/MgO$ and $Fe_3O_4/CoO$ interfaces.

Two magnetite films were grown under conditions where a half-filled *A*-site termination at the surface is expected. During and after the growth of the $Fe_3O_4$ film we observed from RHEED a $(\sqrt{2}\times\sqrt{2})R45°$ surface symmetry. Deposition of $^{57}Co$ probe atoms changed the surface symmetry to $1\times1$. The change is due to a disordered arrangement of probe atoms at the $Fe_3O_4(100)$ surface. The EMS study of the surface shows that the Fe probe ions at the magnetite surface are in $2+$ and $3+$ charge states, isolated from the electron-exchange process. After annealing at 250 °C the $(\sqrt{2}\times\sqrt{2})R45°$ surface symmetry is recovered. The EMS shows that about one-third of the probe atoms remain at the surface, the rest diffuse into *B* sites below the surface. After the annealing all probe atoms participate in the electron-exchange process. Structural relaxation of the first four surface layers and the reduced number of magnetic neighbors at the surface are responsible for the observed enhanced fluctuations of the spins at and close to the surface.

Deposition of a MgO layer on the magnetite film largely removes the structural relaxation. As a result the fluctuation of the spins at the $Fe_3O_4/MgO$ interface is significantly reduced, although it is still present on the time scale of the Mössbauer measurement ($\sim$100 ns) due to the reduced number of magnetic neighbors at the interface. At 130 K the probe atoms at the $Fe_3O_4/MgO$ interface are found to be in a $Fe^{3+}$ charge state. The presence of divalent Mg neighbors of the *B*-site Fe ions might create a potential barrier at the interface which at 130 K isolates the interface probe atoms from the electron exchange. In contrast, the spins located closely below the interface do not behave different from the bulk of the layer. If the small TMR effect in $Fe_3O_4/MgO/Fe_3O_4$ tunnel junctions has an interface origin it should be associated with the very first monolayer at the interface.

Diffusion of Co into the $Fe_3O_4$ film was observed after deposition of CoO on top of the $Fe_3O_4$ film. This diffusion is responsible for the formation of an interface cobalt substituted magnetite layer ($Co_xFe_{3-x}O_4$) between the $Fe_3O_4$ and CoO layers. We estimate the cobalt content *x* of this interface layer to be $0.5\pm0.1$.

## ACKNOWLEDGMENTS

The authors would like to acknowledge L. Venema, H. E. Kielman, F. Th. ten Broek, and J. J. Smit for the technical assistance in performing the soft-landing experiment.

[1] R.M. Wolf, A.E.M. De Veirman, P. van der Sluis, P.J. van der Zaag, and J.B.F. aan de Stegge, in *Epitaxial Oxide Thin Films and Heterostructures*, edited by D.K. Fork, J.M. Phillips, R. Ramesh, and R.M. Wolf, MRS Symposia Proceedings No. 23 (Materials Research Society, Pittsburgh, 1994), p. 341.

[2] T. Hibma, F.C. Voogt, L. Niesen, P.A.A. van der Heijden, W.J.M. de Jonge, J.J.T.M. Donkers, and P.J. van der Zaag, J. Appl. Phys. **85**, 5291 (1999).

[3] R. Cornell and U. Schwertmann, *The Iron Oxides* (Verlagsgellschaft, Cambridge, 1996).

[4] C. Srinitiwarawong and G.A. Gehring, J. Phys.: Condens. Matter **13**, 7987 (2001).

[5] H. Feil, Ph.D. thesis, University of Groningen, 1987; H. Feil, Solid State Commun. **69**, 245 (1989).

[6] X.W. Li, A. Gupta, Gang Xiao, W. Qian, and V.P. Dravid, Appl. Phys. Lett. **73**, 3282 (1998).

[7] P.J. van der Zaag, P.J.H. Bloemen, J.M. Gaines, R.M. Wolf, P.A.A. van der Heijden, R.J.M. van de Veerdonk, and W.J.M. de Jonge, J. Magn. Magn. Mater. **211**, 301 (2000).

[8] P.W. Tasker, J. Phys. C **12**, 4977 (1979).

[9] P.W. Tasker, Philos. Mag. A **12**, 4977 (1979).

[10] G. Tarrach, D. Buergler, T. Schaub, R. Wiesendanger, and H.-J. Guentherodt, Surf. Sci. **285**, 1 (1993).

[11] F.C. Voogt, T. Hibma, G.L. Zhang, M. Hoefman, and L. Niesen, Surf. Sci. **331-333**, 1508 (1995).

[12] F.C. Voogt, T. Fujii, P.J.M. Smulders, L. Niesen, M.A. James, and T. Hibma, Phys. Rev. B **60**, 11 193 (1999).

[13] B. Stanka, W. Hebenstreit, U. Diebold, and S.A. Chambers, Surf. Sci. **448**, 49 (2000).

[14] S.A. Chambers, S. Thevuthasan, and S.A. Joyce, Surf. Sci. Lett. **450**, L273 (2000).

[15] A.V. Mijiritskii and D.O. Boerma, Surf. Sci. **486**, 73 (2001).

[16] J. Korecki, B. Handke, N. Spiridis, T. Slezak, I. Flis-Kabulska, and J. Haber, Thin Solid Films **412**, 14 (2002).

[17] G. Mariotto, S. Murphy, and I.V. Shvets, Phys. Rev. B **66**, 245426 (2002).

[18] J.M.D. Coey, I.V. Shvets, R. Wiesendanger, and H.-J. Guentherodt, J. Appl. Phys. **73**, 6742 (1993).

[19] D.M. Lind, S.D. Berry, G. Chern, H. Mathias, and L.R. Testardi, Phys. Rev. B **45**, 1838 (1992).

[20] P.A.A. van der Heijden, J.J. Hammink, P.J.H. Bloemen, R.M. Wolf, M.G. van Opstal, P.J. van der Zaag, and W.J.M. de Jonge, in *Magnetic Ultrathin Films, Multilayers, and Surfaces*, edited by A. Feit, H. Fujimori, G. Guntherodt, B. Heinrich, W.F. Egelhoff, Jr., E. E. Marinero, and R. C. White, MRS Symposia Proceedings No. 384 (Materials Research Society, Pittsburgh, 1995), p. 27.

[21] C. Noguera, J. Phys.: Condens. Matter **12**, R367 (2000).

[22] C. Noguera, A. Pojani, P. Casek, and F. Finocchi, Surf. Sci. **507-510**, 245 (2002).

[23] C. Boekema, R.L. Lichti, K.C.B. Chan, V.A.M. Brabers, A.B. Denison, D.W. Cooke, R.H. Heffner, R.L. Hutson, and M.E. Schillaci, Phys. Rev. B **33**, 210 (1986).

[24] F. Walz, J. Phys.: Condens. Matter **14**, R285 (2002).

[25] R.S. Hargrove and W. Kuendig, Solid State Commun. **8**, 303 (1970).

[26] J.M.D. Coey, A.H. Morrish, and G.A. Sawatzky, J. Phys. (Paris), Colloq. **32**, 271 (1971).

[27] H. Annersten and S.S. Hafner, Z. Kristallogr. **137**, 321 (1973).

[28] E. De Grave, R. Leyman, and R. Vandenberghe, Phys. Lett. **97A**, 354 (1983).
[29] J. Delepine, B. Hannoyer, F. Varret, and M. Lenglet, Hyperfine Interact. **28**, 721 (1986).
[30] C.R. Laurens, L. Venema, G.J. Kemerink, and L. Niesen, Nucl. Instrum. Methods Phys. Res. B **129**, 429 (1997).
[31] C.R. Laurens, Ph.D. thesis, University of Groningen, The Netherlands, 1997.
[32] M.F. Rosu, C.R. Laurens, A. Falepin, M.A. James, M.H. Langelaar, F. Pleiter, O.C. Rogojanu, and L. Niesen, Phys. Rev. Lett. **81**, 4680 (1998).
[33] P.J.H. Bloemen, P.A.A. van der Heijden, R.M. Wolf, J. aan de Stegge, J.T. Kohlhepp, A. Reinders, R.M. Jungblut, P.J. van der Zaag, and W.J.M. de Jonge, in *Epitaxial Oxide Thin Films II*, edited by D.K. Fork, J.S. Speck, T. Shiosaki, and R.M. Wolf, MRS Symposia Proceedings No. 401 (Materials Research Society, Pittsburgh, 1996), p. 485.
[34] S.A. Chambers and S.A. Joyce, Surf. Sci. **420**, 111 (1999).
[35] J.M. Gaines, J.T. Kohlhepp, J.T.W. van Eemeren, R.J.G. Elfrink, F. Roozeboom, and W.J.M. de Jonge, in *Epitaxial Oxide Thin Films III*, edited by D.G. Schlom, C.-B. Eom, M.E. Hawley, C.M. Foster, and J.S. Speck, MRS Symposia Proceedings No. 474 (Materials Research Society, Pittsburgh, 1997), p. 191.
[36] J.F. Anderson, M. Kuhn, U. Diebold, K. Shaw, P. Stoyanov, and D. Lind, Phys. Rev. B **56**, 9902 (1997).
[37] E. De Grave, R.M. Persoons, R.E. Vandenberghe, and P.M.A. de Bakker, Phys. Rev. B **47**, 5881 (1993).
[38] W. Kuendig and R.S. Hargrove, Solid State Commun. **7**, 223 (1969).
[39] R.E. Vandenberghe and E. De Grave, in *Mössbauer Spectroscopy Applied to Inorganic Chemistry*, edited by G.J. Long and F. Grandjean (Plenum Press, New York, 1989), Vol. 3, p. 59.
[40] G.A. Sawatzky and F. van der Woude, J. Phys. (Paris), Colloq. **35**, 47 (1974).
[41] F. Grandjean, in *Mössbauer Spectroscopy Applied to Inorganic Chemistry*, edited by G.J. Long (Ref. 39), Vol. 2, p. 241.
[42] D.T. Margulies, F.T. Parker, F.E. Spada, R.S. Goldman, J. Li, R. Sinclair, and A.E. Berkowitz, Phys. Rev. B **53**, 9175 (1996).
[43] L.A. Kalev and L. Niesen, Phys. Rev. B **67**, 224403 (2003).
[44] R.M. Persoons, E. De Grave, P.M.A. de Bakker, and R.E. Vandenberghe, Phys. Rev. B **47**, 5894 (1993).